

## Research Article

# Two-Speed DCT Electric Powertrain Shifting Control and Rig Testing

**Bo Zhu,<sup>1,2</sup> Nong Zhang,<sup>1</sup> Paul Walker,<sup>1</sup> Wenzhang Zhan,<sup>2</sup>  
Xingxing Zhou,<sup>1</sup> and Jiageng Ruan<sup>1</sup>**

<sup>1</sup> University of Technology, Sydney, Ultimo, NSW 2007, Australia

<sup>2</sup> BAIC Motor Electric Vehicle Co. Ltd., DaXing District, Beijing 102606, China

Correspondence should be addressed to Bo Zhu; zhubo2006@126.com

Received 14 August 2013; Revised 4 November 2013; Accepted 4 November 2013

Academic Editor: Xiaosong Hu

Copyright © 2013 Bo Zhu et al. This is an open access article distributed under the Creative Commons Attribution License, which permits unrestricted use, distribution, and reproduction in any medium, provided the original work is properly cited.

Dual clutch transmissions (DCTs) are recognized as being suitable for electric drive applications as they can drive with high efficiency and achieve good shifting comfort. A two-speed DCT electric drivetrain is described in this paper, comprised of only two gear pairs and a final drive gear in the two-speed gearbox. The fundamental shifting control algorithm is provided. On the testing rig of University of Technology, Sydney (UTS) powertrain lab, shifting controls and some driving cycle controls were realized. The results demonstrated that the control algorithm functioned well both in transient shifting control process and in the driving cycle conditions.

## 1. Introduction

The single reducer drivetrain is the most popular transmission structure for Pure Electric Vehicle (PEV) recently, as it uses the wide speed range of electric motor to realize all driving speeds of the vehicle and also provides necessary high torque at low speed for acceleration and grade climbing. But in the development of electric vehicles, it is hard to satisfy the requirement of dynamic performance of PEVs and meet the needed speed range, particularly for some luxury vehicles. More and more, researches and applications are beginning to investigate the applications of multigear transmissions used in PEVs [1].

The application of multigear transmissions for PEVs has the potential to improve average motor efficiency and enhance running range or even reduce the required motor size [2]. However if conventional gearbox, such as automatic transmission (AT), is selected, the powertrain structure will be more complex with hydraulic clutch control system, and the overall efficiency of powertrain may decrease. Additionally, the application of automated manual transmission (AMT) will result in torque interruption during shifting, significantly degrading the ride comfort.

Dual clutch transmissions (DCTs) which use two clutches with a common drum system assembled between the engine and the transmission overcome the shortcomings of the single clutch version [1]. DCTs combine high efficiency of MTs with convenience of automatic transmissions by simultaneously changing between two primary clutches for gear changes. Consequently shift quality and driving comfort can be significantly improved in comparison to MTs, thus making DCTs well suited to applications in PEV powertrains.

In spite of such advantages, controllability plays a crucial role in determining overall performance of DCTs. The clutch-to-clutch shifting process is controlled to achieve a very short inertia phase time which is very important for shift performance. There are some current researches on the modeling and analysis of dynamic characteristics of DCTs [2–6]. The methods suggested in several papers include open-loop based control and PID based control with experimental calibration [6, 7]. Both methods present different opportunities and challenges; open-loop methods are computationally more efficient and require limited calibration by having deficiencies in extreme operating conditions, where calibration may not be sufficient, whereas closed-loop control is comparatively

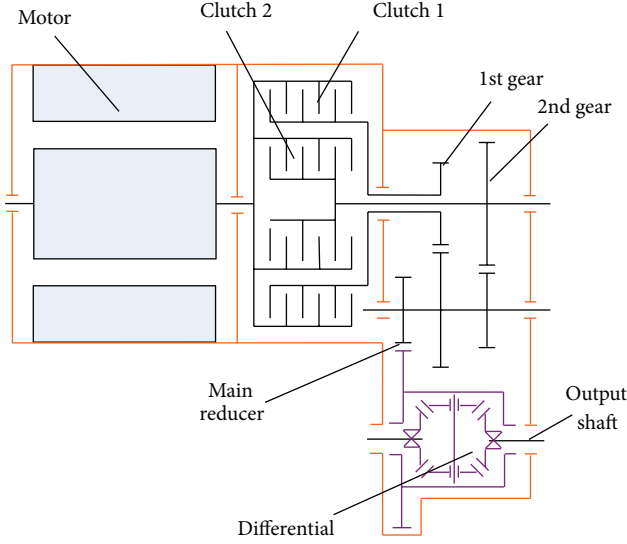


FIGURE 1: Two-speed DCT electric powertrain.

more computationally intensive and requires significant calibration time but is more robust and more likely to continually produce high quality gear shifts over a broad range of operating conditions.

The purpose of this paper is to experimentally investigate the applications of two-speed transmissions for electric vehicles, with particular consideration to gear shift control and its evaluation for different driving cycles, as such, this paper studies open-loop control method of DCT shifting process under PEV system; an upshifting and downshifting algorithm was described. To validate the control algorithm, test rig was built in UTS powertrain lab. Both transient shifting control and driving cycle control were implemented on the test bed. The testing results demonstrated the correctness of the control method for two-speed EVs. It provides theoretical support for PEV powertrain equipped with DCT.

## 2. Two-Speed DCT Pure Electric Powertrain Structure

Figure 1 presents the structure of a front wheel drive two-speed DCT electric vehicle powertrain. It is comprised of motor, coupled clutches, transmission gear train, differential, and output shaft to wheels. The uniqueness of DCT powertrain is the application of clutches and arrangement of gear train. The two clutches have a common drum attached to the input shaft from the motor, and the friction plates are independently connected to the first and second gears, respectively. With only two gear pairs and a final drive gear in the two-speed gearbox it is a comparatively simple transmission, without the requirement to engage alternate gears using synchronizer mechanisms [8, 9]. For just two gear ratios, gear shifting is realized through dual clutch control alone. Additionally, as the motor has the capability to reverse rotation, it can reverse the vehicle; thus the reverse shaft is also eliminated. As a result, the two-speed dual clutch

transmission which equipped EV powertrain is relatively simple.

The simplified powertrain is schematically shown in Figure 2 with clutches in the slip state, consistent with both clutches energized during general shifting conditions. The motor inertia takes input in the form of motor torque and outputs it to the clutch drum via shaft stiffness and damping element. The clutches are coupled to drum so there are two possible torque paths available as inputs that transmit power from the motor and clutch drum, as well as two outputs that drive the gear set either separately or simultaneously. The transmission transfers the clutch output torques to the propeller shaft, where it drives the vehicle inertia which is subjected to various loads such as air drag and rolling resistance. The equations of motion of the open model are

$$I_M \ddot{\theta}_M = K_D (\theta_D - \theta_M) + C_D (\dot{\theta}_D - \dot{\theta}_M) - T_M, \quad (1)$$

$$I_D \ddot{\theta}_D = -K_D (\theta_D - \theta_M) - C_D (\dot{\theta}_D - \dot{\theta}_M) + T_{C1} + T_{C2}, \quad (2)$$

$$I_T \ddot{\theta}_T = K_T (\theta_V - \theta_T) + C_T (\dot{\theta}_V - \dot{\theta}_T) - \gamma_1 T_{C1} - \gamma_2 T_{C2}, \quad (3)$$

$$I_V \ddot{\theta}_V = -K_T (\theta_V - \theta_T) - C_T (\dot{\theta}_V - \dot{\theta}_T) + T_V, \quad (4)$$

where  $\theta$  and its two derivatives are the rotational displacement, velocity, and acceleration, respectively,  $\gamma$  presents the gear ratio,  $I$  is the inertia element,  $C$  is damping coefficient,  $K$  is stiffness coefficient, and  $T$  is torque. For subscripts  $M$  represents motor,  $D$  is clutch drum,  $T$  is transmission,  $V$  is the vehicle,  $C$  is clutch and 1 and 2 represents the two clutches and respective gears. When either of the two clutches is locked, the vehicle reverts to a three-degree-of-freedom model, where the closed clutch merges the inertia of the drum with the transmission via a reduction gear; this gear ratio is the combination of both transmission ratio and final drive ratio for this model.

The equations of motion of the closed model are

$$I_M \ddot{\theta}_M = K_D (\gamma_1 \theta_T - \theta_M) + C_D (\gamma_1 \dot{\theta}_T - \dot{\theta}_M) - T_M,$$

$$(I_D + \gamma_1^2 I_T) \ddot{\theta}_D = \gamma_1 K_D (\gamma_1 \theta_T - \theta_M) - \gamma_1 C_D (\gamma_1 \dot{\theta}_T - \dot{\theta}_M)$$

$$+ K_T (\theta_V - \theta_T) - C_T \dot{\theta}_T + \left(1 \frac{\gamma_2}{\gamma_1}\right) T_{C2},$$

$$I_V \ddot{\theta}_V = -K_T (\theta_V - \theta_T) - C_T (\dot{\theta}_V - \dot{\theta}_T) + T_V. \quad (5)$$

The use of piecewise clutch models to account for transitions between dynamic and static frictions is performed by [2, 8], where, upon clutch synchronization, an algorithm estimates the clutch torque and compares it to static friction to determine if friction lock is successful. A similar model is adopted by [4]; however the postlockup torque is not well defined. In Goetz et al. [7, 10] a transfer function model of the hydraulic system is utilized over a detailed model, citing issues with the discontinuous contact in the clutch as a limiting factor. In this paper a nonlinear spring contact model is used to overcome this issue; thus a fourth variable of

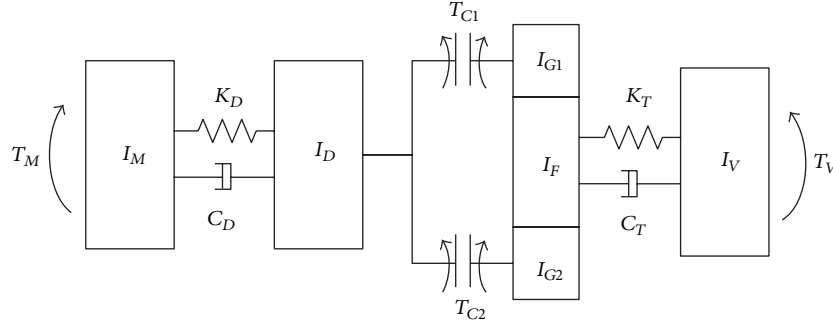


FIGURE 2: Dynamic model of pure electric DCT.

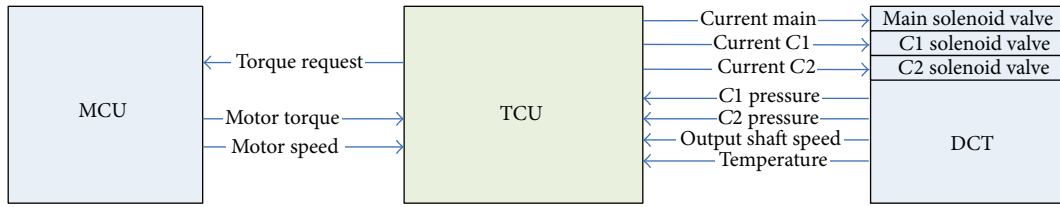


FIGURE 3: Control scheme for the powertrain.

piston displacement is introduced to the piecewise model of the clutch, where the return spring separates the plate contact and the clutch torque drops to zero, excluding a small viscous contact component.

The piecewise model of the clutch is defined as a combination of dynamic and static friction, where the static friction is calculated as the average torque in the clutch, and limited to the static friction of the clutch. This is defined as follows:

$$T_C = \begin{cases} 0, & X < X_0, \\ n\mu_D \frac{r_O^3 - r_I^3}{r_O^2 - r_I^2} \times F_A, & X \geq X_0, |\Delta\dot{\theta}| \geq 0^*, \\ T_{\text{avg}}, & X \geq X_0, |\Delta\dot{\theta}| < 0^*, T_{\text{avg}} < T_{C,S}, \\ n\mu_S \frac{r_O^3 - r_I^3}{r_O^2 - r_I^2} \times F_A, & X \geq X_0, |\Delta\dot{\theta}| < 0^*, T_{\text{avg}} \geq T_{C,S}, \end{cases} \quad (6)$$

where  $n$  is the number of friction plates,  $X$  is piston displacement,  $X_0$  is the minimum displacement required for contact between friction plates,  $\mu_D$  is dynamic friction,  $\mu_S$  is static friction,  $r_O$  and  $r_I$  are the outside and inside diameters of the clutch plates, and  $F_A$  is the pressure load on the clutch. A relatively simple model of the coefficient of friction of the clutches is presented as having dynamic friction,  $\mu_D$ , a static friction,  $\mu_S$ , for an absolute clutch speed of approximately zero, such that numerical error in calculations is eliminated without negatively affecting results, including the phenomena of stick-slip.

With the average torque,  $T_{\text{avg}}$  being derived from the open clutch equations for each of the two engaged clutches as:

$$T_{\text{avg}} = \frac{(T_{CD1,2} + T_{CT1,2})}{2}, \quad (7)$$

$$T_{CD1,2} = 1I_D\ddot{\theta}_D - K_D(\theta_D - \theta_M) - C_D(\dot{\theta}_D - \dot{\theta}_M) - T_{C2,1}, \quad (8)$$

$$T_{CT1,2} = \frac{(I_T\ddot{\theta}_T + K_T(\theta_V - \theta_T) + C_T(\dot{\theta}_V - \dot{\theta}_T) + \gamma_{2,1}T_{C2,1})}{\gamma_{1,2}}, \quad (9)$$

where (8) and (9) are realized by rearranging (2) and (3), respectively. Determining the average torque for clutch 1 or clutch 2 is achieved by using the alternate subscripts of 1 and 2 in sequential order. The average torque is important for torque based control of dual clutch transmissions as it is the target for the engaging clutch control in torque based control applications.

### 3. Shifting Control

The basic form of the control scheme is presented in Figure 3 for shift control. Transmission control unit (TCU) accepts motor torque and speed from motor control unit (MCU), Clutch 1 (C1) pressure, Clutch 2 (C2) pressure, DCT output shaft speed and temperature from DCT. Clutch 1 and Clutch 2 slip values are calculated using motor speed and DCT output shaft speed. During shifting, TCU calculates the C1, C2, and main solenoid valve's control current, through the current control to control C1, C2 pressure and realize shifting process. In the meantime, the motor torque request value should be calculated and control the motor torque changing to achieve smooth shifting effect.

Briefly, DCT shift control is split into torque phase and inertia phase. The purpose of the torque phase is to seamlessly hand dynamic friction torque from the originally engaged clutch to the clutch that is the target for engagement. Towards the end of torque phase control must perform the tasks [11],

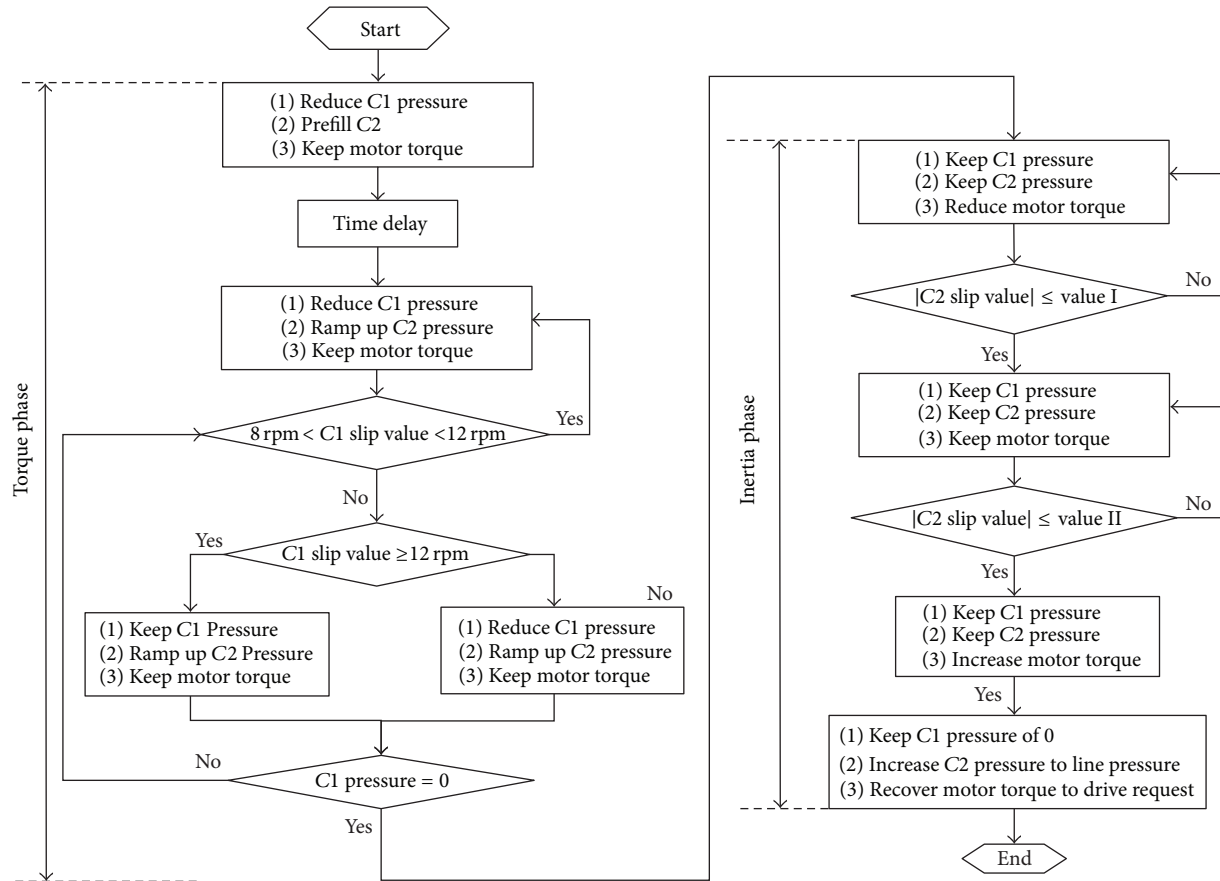


FIGURE 4: Control algorithm for upshifting (C1: the first clutch; C2: the second clutch).

determine the target torque at which the releasing clutch will transit from stick to slip states. Determine the required torque at the engaging clutch required to maintain the acceleration of the vehicle with minimum loss of tractive load, and transfer the torque from the releasing clutch to the engaging clutch in a manner that minimizes vehicle transients.

The inertia phase begins once the target torque has been met during the torque phase. Control and then proceed as follows [11], determine the target torque for the engaging clutch, hold pressure at desired torque, and when speeds are matched, set pressure to maximum and lock the clutch. For the adoption of a torque orientated control strategy in DCT control the inertia phase of control requires that the clutch torque is maintained at a constant torque that is equivalent to the vehicle angular acceleration and any resistance torque. Though it is possible to use higher torques to reduce the shift times, this is likely to result in surging or more significant powertrain transients than it is desirable during shifting in lightly damped powertrains.

**3.1. Upshift Control.** As presented, the control algorithm in Figure 4, at the beginning of power-on upshift, clutch 1 pressure is reduced and clutch 2 is pre-filled resulting in the initiation of slip in clutch 1. After a short time delay, torque transfer begins with clutch 1 slip compensation control. The purpose

of this is to control clutch 1 slip at a given value to guarantee output torque without generating transient shock. The slip value recommended in the literature [12] is 5 rpm, for it is impossible to control the slip in a constant value; a slip zone of 8–12 rpm is selected in this control through calibration.

When clutch 1 pressure decreases down to zero, the torque phase finishes and inertial phase begins. A simple sectional torque control algorithm is studied in this paper. When motor speed synchronizes with clutch 2 speed, then increases clutch 2 pressure to line pressure, and recovers motor torque to drive request value, the shifting process finishes. The process of speed synchronization is divided into three sections; the first section is that when  $C2$  slip value  $\geq$  value I, motor torque is reduced. The second section is when value I  $<$  C2 Slip value  $<$  value II, motor torque is maintained at the desired output value. The third section is that when C2 slip value  $\geq$  value II, motor torque begins to increase again. Here the parameters value I and value II both need to be calibrated. When the motor torque reduces, the output torque of the vehicle is inevitably going to decrease. To avoid large negative jerk in the shift transfer, an appropriate minimum torque limit should be included.

**3.2. Downshift Control.** The power-on downshift process is the opposite to that of power-on upshifting; it begins with

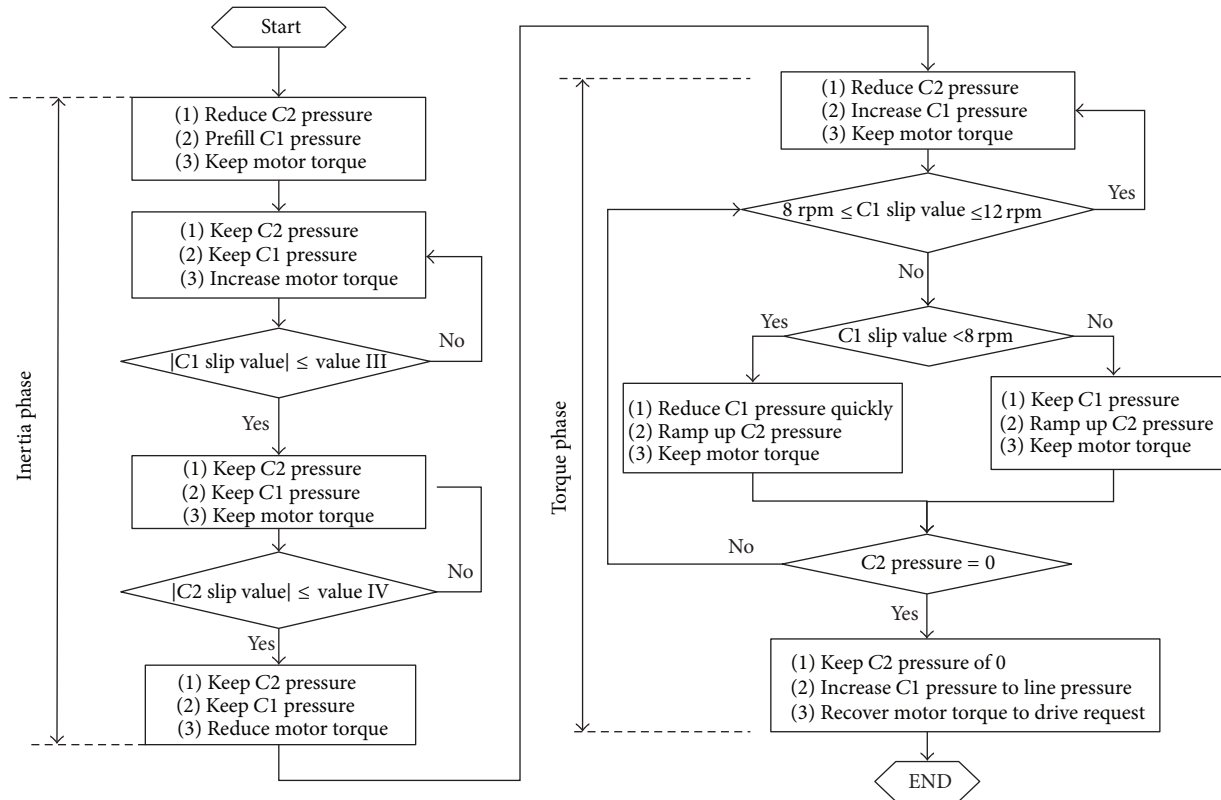


FIGURE 5: Control algorithm for downshift (C1: the first clutch; C2: the second clutch).

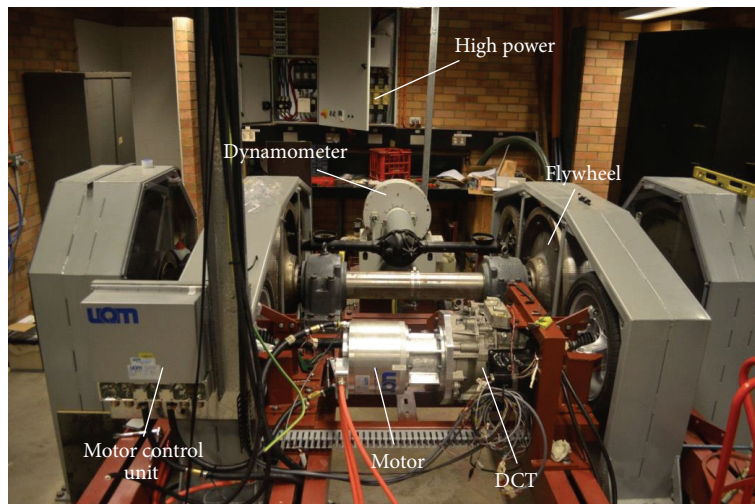


FIGURE 6: Powertrain rig in UTS.

inertial phase. As shown in the control algorithm in Figure 5, firstly clutch 2 pressure is reduced and clutch 1 is prefilled; pressure is set to initiate slip of clutch 2. For down shifting from the 2nd gear to the 1st gear, the speed of motor will increase to synchronize the clutch 1 speed. If the motor torque is less than maximum output value, an increasing torque requirement can be given to shorten the inertial phase. The algorithm is the same as in inertial phase of power-on upshift control; parameters of value III and value IV are selected

and calibrated. When the motor speed has been synchronized with clutch 1 speed, inertial phase finishes and torque phase starts.

In the torque phase, clutch 2 pressure is reduced and clutch 1 pressure is ramped up; also the same slip feedback compensation control as in power-on upshift control is adopted here, to control clutch 1 slip value in the given target value during torque transfer ensuring smooth shifting. While clutch 2 pressure is reduced to zero and increases clutch 1

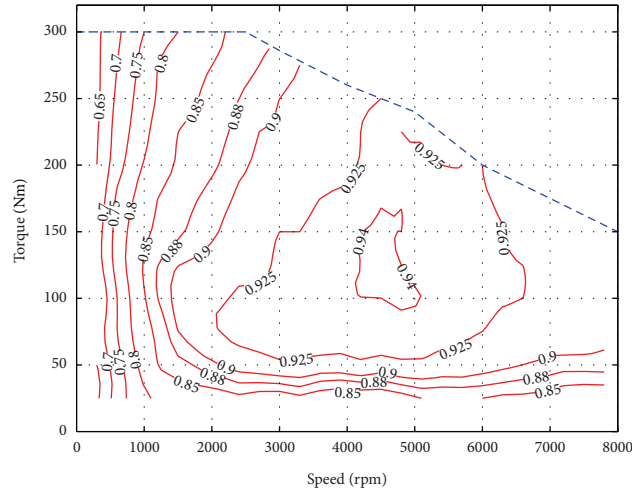
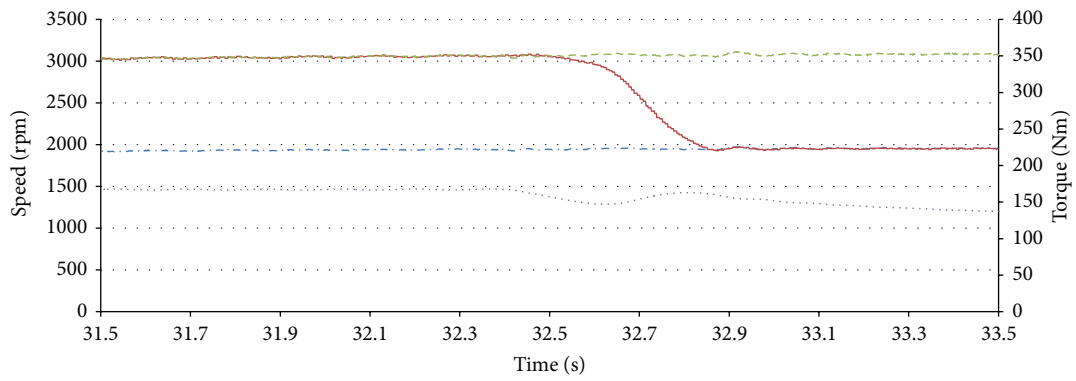
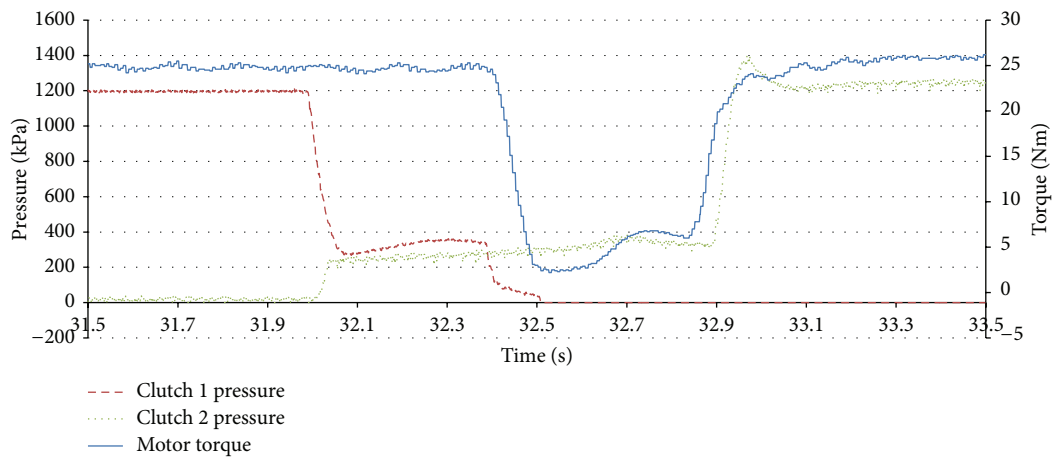


FIGURE 7: Motor efficiency of MAP.

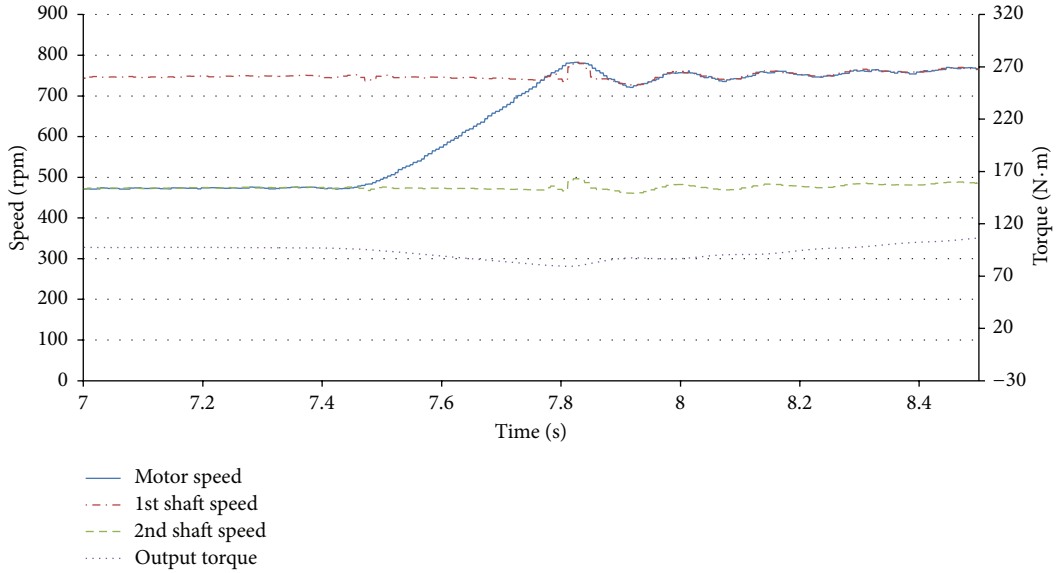


(a)

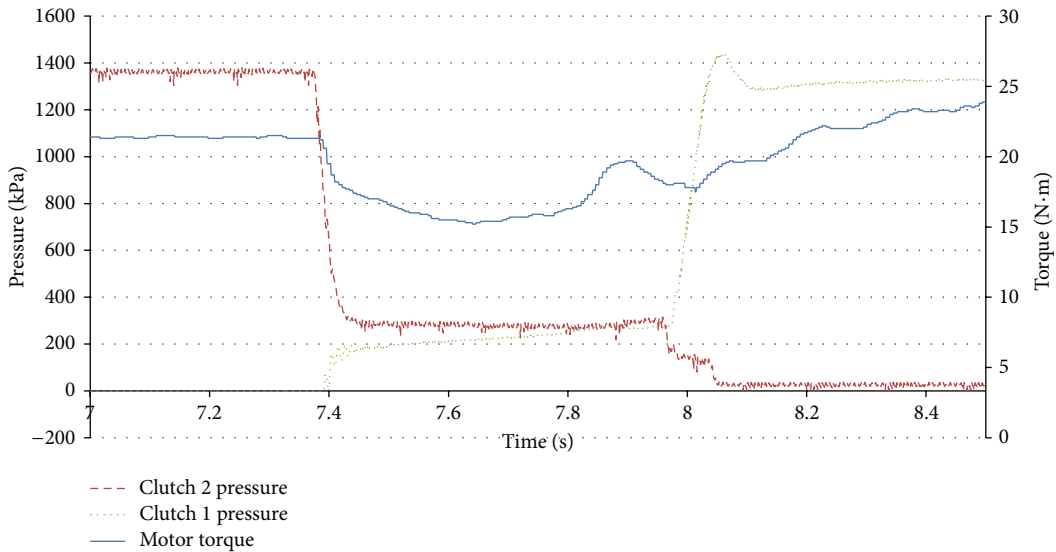


(b)

FIGURE 8: Upshift results (3000 rpm 25 Nm).



(a)



(b)

FIGURE 9: Downshift results (500 rpm 25 Nm).

pressure to line pressure, the shifting process completes and motor torque is recovered to driver demand values.

#### 4. Testing Rig

For the two-speed DCT development and control calibration, test rig was transformed from UTS powertrain rig. The rig after modification is shown in Figure 6. Resistant torques for the rig are developed using an eddy-current dynamometer. The vehicle mass is represented with four big flywheels to simulate the rolling inertia and two pairs of wheels are used to transmit torque from powertrain to flywheels and from flywheels to dynamometer. The powertrain is the motor and DCT; it consists of a two-speed DCT and drive motor.

A 125 kW PM motor was selected on the test rig. The max torque of motor was 300 Nm, Figure 7 is the motor efficiency MAP which included the efficiency of motor and controller. There is no battery in the rig; a high voltage DC power is used with 380 V to provide power to drive the powertrain. To test economic performance of the system, a simulated SOC value was calculated by DC current and voltage in software:

$$SOC = SOC_0 - \frac{1}{3.6 * B_C * B_V} \int \frac{V * I}{1000} dt, \quad (10)$$

where  $SOC_0$  is initial value (here we set it as 95%),  $B_C$  is battery capacity, which is 72 Ah here, and  $B_V$  is battery rate voltage, which is 380 V and equal to DC power voltage.  $V$  and  $I$  are real voltage and current value input from DC bus.

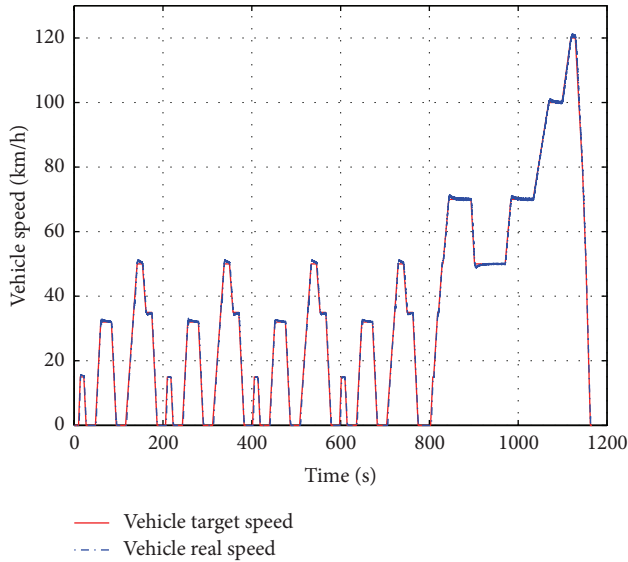


FIGURE 10: NEDC driving cycle.

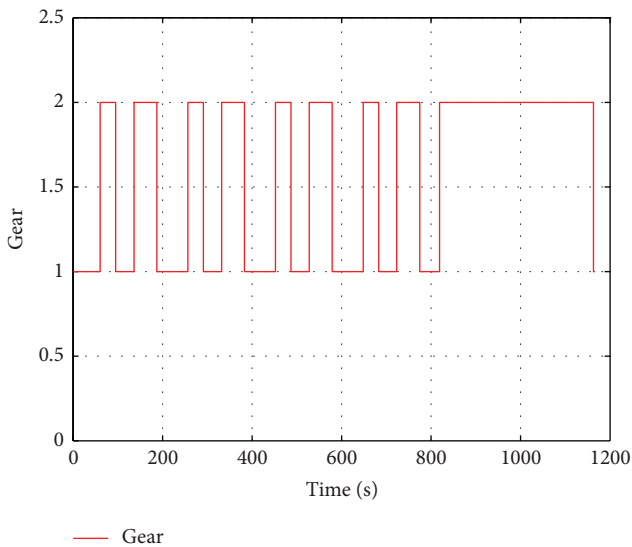


FIGURE 11: Gear in NEDC.

This test rig is different from the normal single dynamometer testing system and also different from the conventional double dynamometer double output shaft transmission test bed. Its two-shaft coupling structure can satisfy front engine and front drive (FF) powertrain testing with only single dynamometer. The powertrain is easy to mount and will not have the alignment problem. The flywheels simulated vehicle inertial, also with four wheels on the rig to simulate real wheel on vehicle; consequently the powertrain is capable of producing transient response testing more close to real situations. It can satisfy most of the transient performance testing and control parameter calibration.

## 5. Testing Results

To validate and test the two-speed DCT and control system, both transient and steady-state experiments were completed on the rig. The transient test was utilized to demonstrate the control effects, upshift control results are presented in Figure 8, and downshift control results are presented in Figure 9, in which, (a) is speed changing process of the motor and the total gearbox output torque and (b) are pressures of clutch 1 and clutch 2, with the motor torque changing during shifting.

In Figure 8(a), from 31.9 s to 32.4 s is the torque phase, C1 pressure reduces to 300 kPa, and C2 pressure prefills to 250 kPa. After that, in inertial phase motor torque decreases from 25 Nm to 5 Nm; in the meantime motor speed synchronizes to C2 speed. When the speed synchronization finishes, motor torque recovers to drive's requirement.

Downshift control results are presented in Figure 9. It begins with inertial phase during which C2 pressure decreases to 300 kPa, and C1 pressure prefills and keeps the value of 200 kPa. Motor torque decreases from 22 Nm to 15 Nm, when motor speed synchronizes to C1 speed, increases motor torque. Then in the torque phase, C2 pressure reduces to 0 and C1 pressure ramps up.

From both Figures 8 and 9, the shifting process is smooth; there is only a little output torque vibration, without torque hole. The motor speeds synchronize with the target speed stably. Torque and speed transients are relatively small providing qualitative assessment of good shift quality in the powertrain.

Furthermore, to validate the economic performance, driving cycle tests are used to judge energy consumption and running distance for a given range of battery SOC. In this paper selected cycles are new european driving cycle (NEDC) and urban dynamometer driving schedule (UDDS). The NEDC is regulated European cycle for defining the specific fuel consumption and emissions of passenger cars. Entire cycle includes four ECE segments, followed by one EUDC segment (Figure 10). Its average speed is 33.6 km/h, the maximum speed is 120 km/h, and the total distance is 11 km. UDDS is also known as the US FTP-72 (Federal Test Procedure) or the LA-4 cycle. It is simulation of an urban driving route approximately 12.1 km (7.4 miles) long and takes 1,369 seconds (approximately 23 minutes) to complete, as shown in Figure 14. In both Figures 10 and 14, there are two lines; the solid line is the target "vehicle" speed of the running cycle, while the dashed line is the actual running speed. We can see that they are essentially identical, indicating that the powertrain model is capable of meeting required driving patterns.

Figures 11 and 15 show the gear shifting between the first and the second gears during the NEDC and UDDS drive cycles. The benefit of the electric motor is realized in infrequency of gear shifting. Obviously, the advantages of the two-speed transmission result in the reduction peak motor speed and torque in the prescribed drive cycle, demonstrated in Figures 12 and 16.

Figures 13 and 17 are calculated SOC value, decreased from 93.8% to 86.2% in NEDC driving cycle, and 95% to



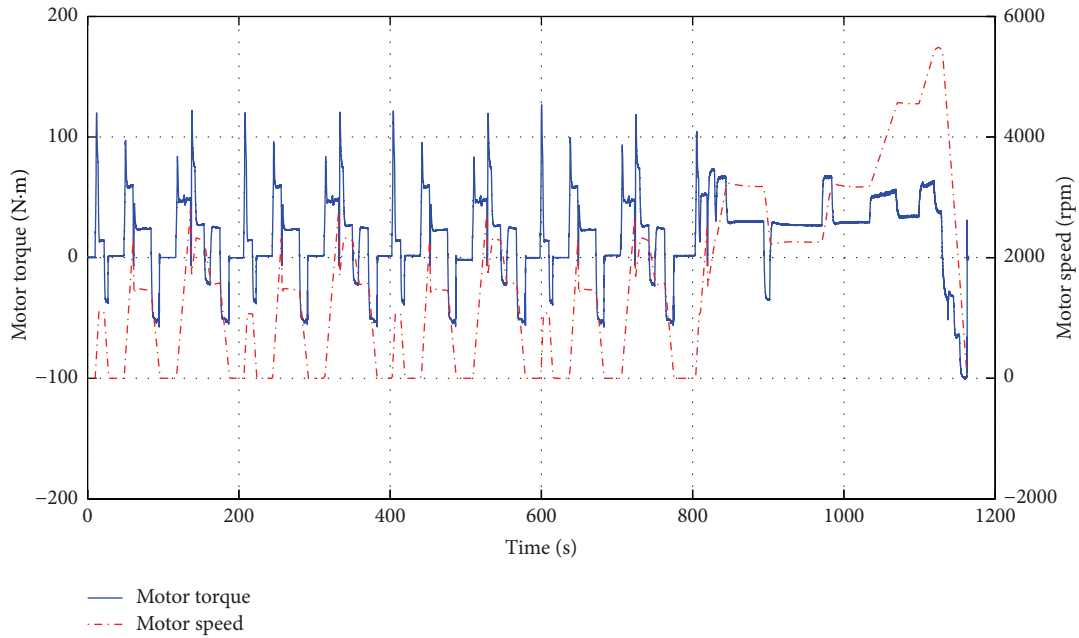


FIGURE 12: Motor speed and torque in NEDC.

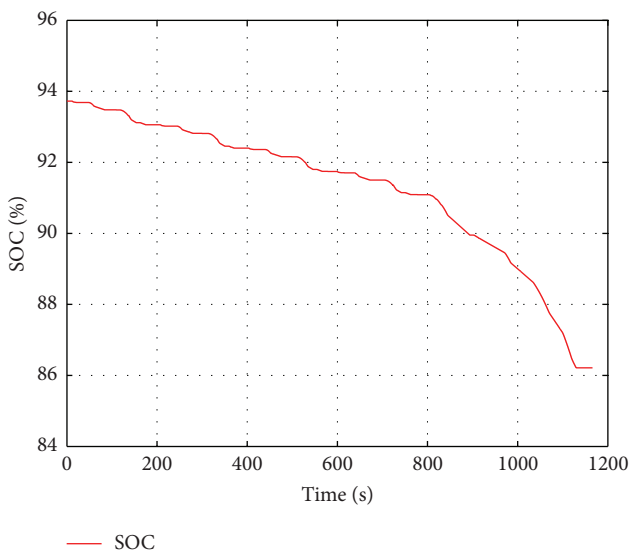


FIGURE 13: SOC in NEDC.

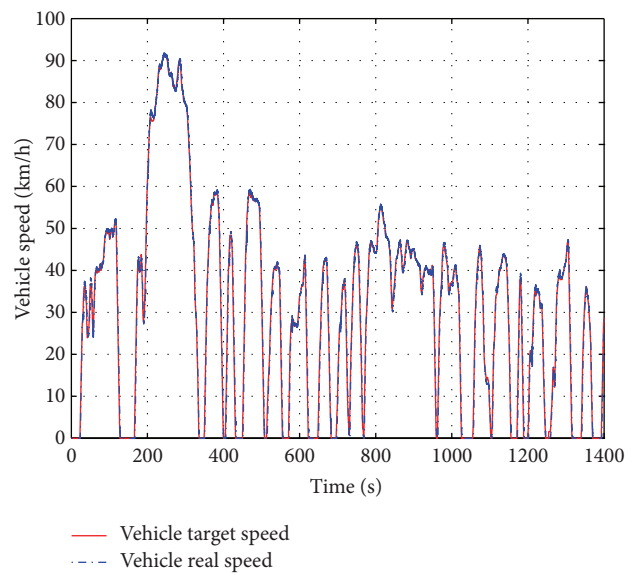


FIGURE 14: UDDS driving cycle.

86.5% in UDDS driving cycle. From SOC we can evaluate the economic performance of the system. From all the result figures above, we can conclude that the two-speed DCT can realize shifting with a good control effect under normal drive cycles.

### 6. Conclusions

To investigate shift control of PEV system equipped with a DCT transmission, a two-speed DCT electric powertrain was developed. Testing rig was modified in UTS powertrain lab to satisfy control calibration and testing. Detailed shifting

control algorithms were developed upshift and downshift control algorithms were demonstrated in the paper. Here just open-loop control algorithm was studied. From the testing results, control program can realize the transient shifting control and get a good transient control performance during the shifting. Open-loop control method is easier than close-loop feedback control, which needs testing calibration to fulfill key factor value settings, such as slip value and pressure changing rate in this control algorithm. The close-loop control algorithm development and testing need more time to process, and will be next step work in the further.

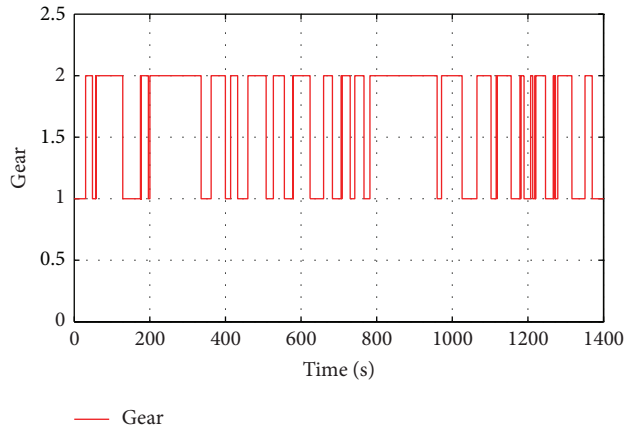


FIGURE 15: Gear in UDDS.

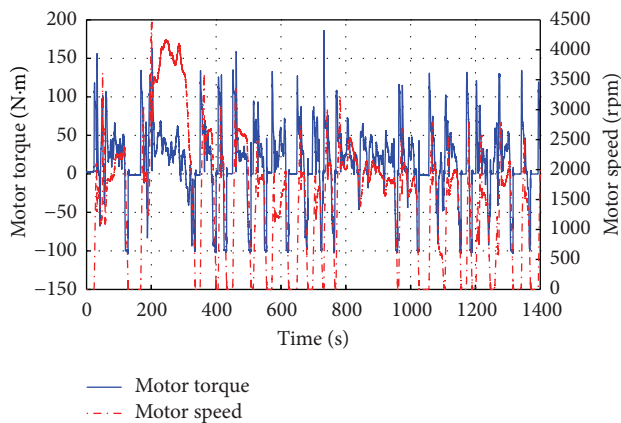


FIGURE 16: Motor speed and torque in UDDS.

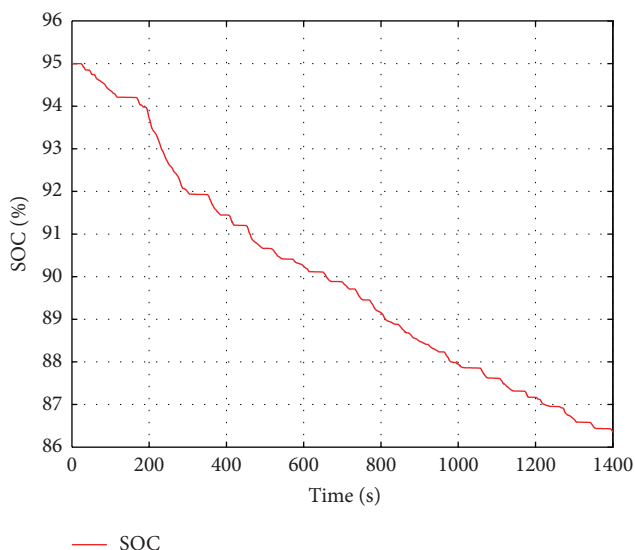


FIGURE 17: SOC in UDDS.

Furthermore driving cycle tests were done on the rig; the typical NEDC and UDDS drive cycles were selected to validate the control program in normal running. The results also showed the good following characteristics of the vehicle speed on the rig: it can simulate the real running conditions well in the lab and can be applied to calibrate control parameters and test performance.

### Conflict of Interests

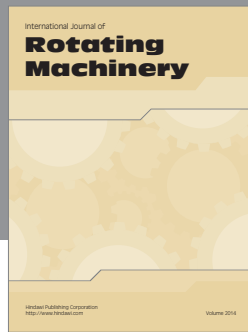
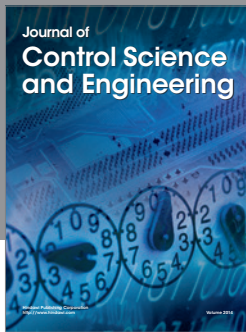
The authors declare that there is no conflict of interests regarding the publication of this paper.

### Acknowledgments

This project is supported by BAIC Motor Electric Vehicle Co. Ltd., the Ministry of Science and Technology, China, and University of Technology, Sydney.

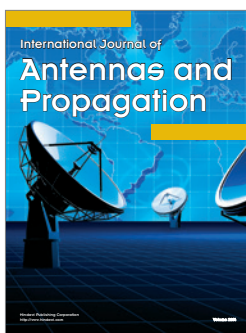
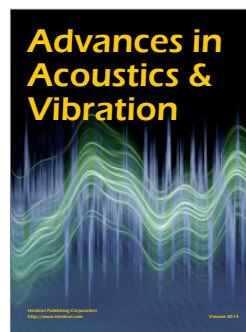
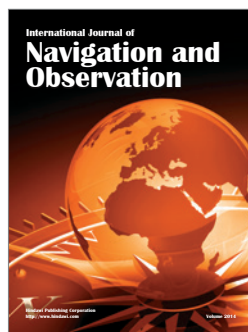
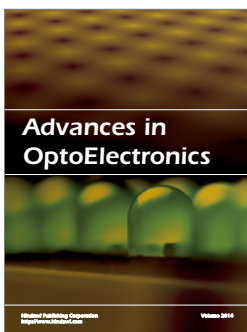
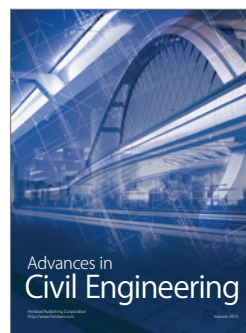
### References




- [1] W. Grobpietsch and T. Sudau, Dual Clutch for Power-Shift Transmissions-A Traditional Engaging Element with New Future, VDI Berichte Nr. 1565, 2000.
- [2] P. D. Walker, N. Zhang, and R. Tamba, "Control of gear shifts in dual clutch transmission powertrains," *Mechanical Systems and Signal Processing*, vol. 25, no. 6, pp. 1923–1936, 2011.
- [3] B. Matthes, "Dual clutch transmissions—lessons learned and future potential," Tech. Rep., SAE, 2005.
- [4] M. Kulkarni, T. Shim, and Y. Zhang, "Shift dynamics and control of dual-clutch transmissions," *Mechanism and Machine Theory*, vol. 42, no. 2, pp. 168–182, 2007.
- [5] S. J. Park, W. S. Ryu, J. G. Song, H. S. Kim, and S. H. Hwang, "Development of DCT vehicle performance simulator to evaluate shift force and torque interruption," *International Journal of Automotive Technology*, vol. 7, no. 2, pp. 161–166, 2006.
- [6] Y. Zhang, X. Chen, X. Zhang, H. Jiang, and W. Tobler, "Dynamic modeling and simulation of a dual-clutch automated lay-shaft transmission," *Transactions of the ASME on Mechanical Design*, vol. 127, no. 2, pp. 302–307, 2005.
- [7] M. Goetz, M. C. Levesley, and D. A. Crolla, "Dynamic modelling of a twin clutch transmission for controller design," *Materials Science Forum*, vol. 440–441, pp. 253–260, 2003.
- [8] P. D. Walker, N. Zhang, W. Z. Zhan, and B. Zhu, "Modeling and simulation of gear synchronization and shifting in dual clutch transmission equipped powertrains," *Proceedings of the Institution of Mechanical Engineers C*, vol. 227, 2013.
- [9] E. Galvagno, M. Velardocchia, and A. Vigliani, "Dynamic and kinematic model of a dual clutch transmission," *Mechanism and Machine Theory*, vol. 46, no. 6, 2011.
- [10] M. Goetz, M. C. Levesley, and D. A. Crolla, "Dynamics and control of gearshifts on twin-clutch transmissions," *Proceedings of the Institution of Mechanical Engineers D*, vol. 219, no. 8, pp. 951–963, 2005.
- [11] P. D. Walker, *Dynamics of powertrains equipped with dual clutch transmissions [Ph.D. thesis]*, University of Technology, Sydney, Australia, 2011.
- [12] M. Goetz, *Integrated powertrain control for twin clutch transmissions [Ph.D. thesis]*, University of Leeds, 2005.



# Hindawi

Submit your manuscripts at  
<http://www.hindawi.com>



▼ Basic Description	
<b>Title</b>	Advances in Mechanical Engineering (New York)
<b>ISSN</b>	1687-8140
<b>Publisher</b>	Hindawi Publishing Corporation
<b>Country</b>	United States
<b>Status</b>	Active
<b>Start Year</b>	2008
<b>Frequency</b>	Continuously
<b>Language of Text</b>	Text in: English
<b>Refereed</b> 	Yes
<b>Abstracted / Indexed</b>	Yes
<b>Open Access</b> 	Yes <a href="http://www.hindawi.com/journals/ame/">http://www.hindawi.com/journals/ame/</a>
<b>Serial Type</b>	Journal
<b>Content Type</b>	Academic / Scholarly
<b>Format</b>	Online
<b>Website</b>	<a href="http://www.hindawi.com/journals/ame">http://www.hindawi.com/journals/ame</a>
► Subject Classifications	
<b>Subject</b>	ENGINEERING - MECHANICAL ENGINEERING 
<b>Dewey #</b>	621
► Additional Title Details	
<b>Key Features</b>	Abstracted or Indexed
	Available Online
	Open Access
	Refereed / Peer-reviewed
► Publisher & Ordering Details	
<b>Commercial Publisher</b>	
Hindawi Publishing Corporation	
Address: 410 Park Ave, 15th Fl, PMB 287, New York, NY 10022 United States	
Fax: 215-893-4392	
Website: <a href="http://www.hindawi.com">http://www.hindawi.com</a>	
Email: <a href="mailto:orders@hindawi.com">orders@hindawi.com</a>	
► Abstracting & Indexing	
<b>Abstracting &amp; Indexing Databases</b>	<ul style="list-style-type: none"> <li>• EBSCOhost <ul style="list-style-type: none"> <li>◦ <a href="#">Applied Science &amp; Technology Source</a>, 1/1/2008-</li> <li>◦ <a href="#">Computers &amp; Applied Sciences Complete</a>, 1/1/2008-</li> <li>◦ <a href="#">Current Abstracts</a>, 1/1/2008-</li> </ul> </li> </ul>

- [Engineering Source](#), 1/1/2008-
- [Inspec](#)
- [TOC Premier \(Table of Contents\)](#), 1/1/2008-
- Elsevier BV
  - [Scopus](#), 2010-
- Gale
  - [Academic OneFile](#), 09/2012-
  - [Expanded Academic ASAP](#), 9/2012-
  - [InfoTrac Custom](#), 1/2009-
- Ovid
  - [Inspec](#)
- ProQuest
  - [Abstracts in New Technologies and Engineering \(Online\), Selective](#)
  - [CSA / ASCE Civil Engineering Abstracts \(Cambridge Scientific Abstracts / American Society of Civil Engineers\), Selective](#)
  - [CSA Engineering Research Database \(Cambridge Scientific Abstracts\), Core](#)
  - [Earthquake Engineering Abstracts, Selective](#)
  - [Mechanical & Transportation Engineering Abstracts, Core](#)
  - [ProQuest SciTech Collection](#), 01/01/2009-
- Thomson Reuters
  - [Current Contents](#)
  - [Science Citation Index Expanded](#)

► Other Availability

**Document Delivery Services**

[Linda Hall Library of Science, Engineering & Technology \\*  
Document Delivery Services](#)

**Related Titles**

► Alternative Media Edition (1)



Journal Menu

- About this Journal
- Abstracting and Indexing
- Aims and Scope
- Annual Issues
- Article Processing Charges
- Articles in Press
- Author Guidelines
- Bibliographic Information
- Citations to this Journal
- Contact Information
- Editorial Board
- Editorial Workflow
- Free eTOC Alerts
- Publication Ethics
- Reviewers Acknowledgment
- Submit a Manuscript
- Subscription Information
- Table of Contents

- Open Special Issues
- Published Special Issues
- Special Issue Guidelines

### Article Processing Charges

Open access publishing proposes a relatively new model for scholarly journal publishing that provides immediate, worldwide, barrier-free access to the full-text of all published articles. Open access allows all interested readers to view, download, print, and redistribute any article without a subscription, enabling far greater distribution of an author's work than the traditional subscription-based publishing model. Many authors in a variety of fields have begun to realize the benefits that open access publishing can provide in terms of increasing the impact of their work.

In an open access model, the publication costs of an article are paid from an author's research budget, or by their supporting institution, in the form of Article Processing Charges. These Article Processing Charges replace subscription charges and allow publishers to make the full-text of every published article freely available to all interested readers. In addition, authors who publish in our open access journals retain the copyright of their work, which is released under a "Creative Commons Attribution License," enabling the unrestricted use, distribution, and reproduction of an article in any medium, provided that the original work is properly cited.

Advances in Mechanical Engineering is an Open Access journal. Publishing an article in Advances in Mechanical Engineering requires Article Processing Charges that will be billed to the submitting author upon acceptance of the article for publication in accordance with the following table.

Manuscript Type	APC
Research Article	\$1200
Review Article	\$1200

### Related Journals

You may also be interested in the following related journals.

Journal	APC
Advances in Acoustics and Vibration	Free
Advances in Materials Science and Engineering	\$1200
Chinese Journal of Engineering	Free
Indian Journal of Materials Science	Free
ISRN Materials Science	Free
ISRN Mechanical Engineering	Free
Journal of Computational Engineering	Free
Journal of Engineering	Free
Journal of Materials	Free
The Scientific World Journal	\$1000